Biophysical Chemistry 185 (2014) 14–18

Contents lists available at ScienceDirect

Biophysical Chemistry

journal homepage: http://www.elsevier.com/locate/biophyschem

Thermal stability of quadruplex primers for highly versatile isothermal DNA amplification

Jordan Mathias [1], Robert Okyere, Levan Lomidze, David Gvarjaladze, Karin Musier-Forsyth, Besik Kankia *

Department of Chemistry and Biochemistry, Center for RNA Biology, The Ohio State University, Columbus, OH 43210, USA

HIGHLIGHTS

- Driving force of QPA comes from the thermal stabilities of primer/template and quadruplex.
- Purine bases incorporated at loop positions significantly destabilize the quadruplex.
- 5′-End dinucleotide extension also destabilizes the quadruplex.

GRAPHICAL ABSTRACT

Scheme showing linear QPA, which isothermally amplifies the DNA signal and allows real-time monitoring through incorporated fluorescence nucleotides.

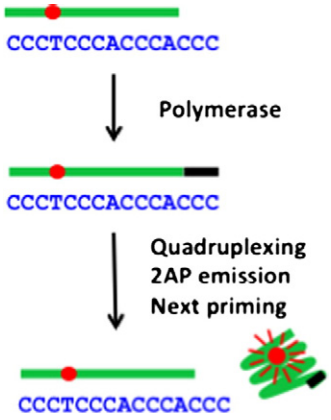

ARTICLE INFO

Article history:
Received 30 September 2013
Received in revised form 30 October 2013
Accepted 30 October 2013
Available online 9 November 2013

Keywords:
DNA quadruplexes
Quadruplex priming amplification
DNA thermodynamics
Thermal unfolding

ABSTRACT

Quadruplex priming amplification (QPA) allows isothermal amplification of nucleic acids with improved yield and simplified detection. This assay is based on a DNA quadruplex, GGGTGGGTGGGTGGG (G3T), which in the presence of specific cations possesses unusually high thermal stability. QPA employs truncated G3T sequences as primers, which upon polymerase elongation, self-dissociate from the binding site and allow the next round of priming without thermal unfolding of amplicons. The rate of amplification strongly depends on the thermal stability of the primer/primer binding site (PBS) complex and to date QPA has been demonstrated to work over a narrow temperature range. To expand the capabilities of QPA, in the present study, we studied the fold and thermodynamic properties of the wild-type G3T and variants containing sequence modifications or extensions at the 5′-end. Circular dichroism studies demonstrate that the substitution of thymidines by other nucleotides or GC addition at the 5′-end does not change the parallel fold of G3T. Thermal unfolding experiments revealed that purine bases incorporated at loop positions and 5′-end dinucleotide extension significantly destabilize the quadruplex, while loop pyrimidines have almost no effect. Overall, the results of these studies suggest that linear isothermal QPA can be performed over a wide temperature range to accommodate both thermophilic and mesophilic DNA polymerases.

* Corresponding author. Tel.: +1 614 688 8799; fax: +1 614 688 5402.
E-mail address: kankia.1@osu.edu (B. Kankia).
[1] Current address: Department of Chemistry and Physics, Armstrong Atlantic State University, 10935 Abercorn Street, Savannah, GA 31419, USA.

0301-4622/$ – see front matter © 2013 Elsevier B.V. All rights reserved.
http://dx.doi.org/10.1016/j.bpc.2013.10.008

1. Introduction

DNA quadruplexes or G-quartets are involved in the regulation of gene expression and are present in telomeres at the ends of chromosomes and in viral RNA systems [1–6]. G-quartets are also found in DNA aptamers [7–10], which are useful in biotechnological and therapeutic applications, as they offer molecular recognition properties that rival that of the commonly used antibodies. G-quartets are formed by four guanine residues, which are associated in a square planar configuration. Each guanine interacts with its two neighbors through Hoogsteen hydrogen bonds. The formation of G-quartets requires the presence of cations, such as K^+, which bind specifically to guanine O6 carbonyl groups between the planes of the G-quartets. Due to this cation coordination and stacking interactions, quadruplexes are remarkably stable and fold readily. This is particularly true for monomolecular quadruplexes, which are formed by stacks of G-quartets connected to each other by single-stranded loops.

One of the most thermally stable quadruplexes is formed by d(GGGTGGGTGGGTGGG) (G3T) [11], which is a truncated version of a DNA aptamer selected for binding to HIV-1 integrase [12]. This sequence folds rapidly into a monomolecular quadruplex with all parallel G-tracts and chain-reversal single-loops [11,13]. In the presence of 50 mM K^+ ions, the melting temperature, T_m, of G3T is ~100 °C, while at the same ionic strength created in the presence of Cs^+ ions (which do not support quadruplex formation), the corresponding duplex unfolds at 60 °C [14]. In addition, removal of one or two guanines from the 3′-end of G3T inhibits quadruplex formation, and shorter duplexes reveal similar values of T_m in the presence of both K^+ and Cs^+ ions [14]. Based on these properties, our laboratory has developed an isothermal DNA amplification assay, quadruplex priming amplification (QPA), which employs truncated G3T sequences as primers [14,15]. Upon polymerase elongation, the primers regain their quadruplex formation capability and due to their unusual thermodynamics, self-dissociate from the target allowing the next round of priming without thermal unfolding of amplicons. As a result, QPA is able to amplify DNA isothermally [14,15], which is critical for DNA-based point-of-care diagnostics [16]. In addition, G3T quadruplex formation represents a convenient molecular switch to turn on intrinsically fluorescent nucleotide analogs, which allows simple and effective quantification of amplicons without extra probe molecules [14,17]. Specifically, 2-aminopurine (2AP) and 6-methylisoxanthopterin (6MI) substituted for thymidines in the 4th, 8th and 12th positions, demonstrated ~80-fold increase in fluorescence upon quadruplex formation [17]. 2AP and 6MI are fluorescent analogs of adenine and guanine, respectively, and are therefore capable of forming Watson–Crick base pairs with thymidine [18,19] and cytosine [20].

Our recent studies revealed that the rate of linear QPA strongly depends on the thermal stability of the primer/PBS complex. Therefore, to perform QPA at different temperatures, primers with different stabilities are needed [15]. We hypothesize that this can be achieved by nucleotide substitution at the loop positions and/or changing the length of the PBS. For example, to conduct QPA at higher temperatures, C or G nucleotides may be incorporated at the loop positions and/or a short oligonucleotide can be appended to the 5′-end. To conduct QPA at a lower temperature, one can use A and T nucleotides at the loop positions and truncate the PBS at the 3′-end. In the present work, to expand the temperature range and versatility of QPA, we systematically studied the effect of nucleotide substitutions in loop positions. We also studied the effect of short attachments and truncations at the 3′-end of the PBS. The results demonstrate that the substitution of loop thymidines or GC attachment at the 5′-end does not change the parallel fold of G3T. Thermal unfolding experiments revealed that purine bases incorporated in loop positions and oligonucleotide attachment at the 5′-end significantly destabilize the quadruplex, while T → C loop substitutions have almost no effect. Overall, these studies suggest that linear QPA can be performed over a wide temperature range suitable for use with both thermophilic and mesophilic DNA polymerases.

2. Materials and methods

DNA oligonucleotides (see Tables 1, 2 and 3) were obtained from Integrated DNA Technologies and Fidelity Systems. The concentration of the DNA oligonucleotides was determined by measuring UV absorption at 260 nm as described earlier [21]. Unless otherwise noted, all measurements were performed in 10 mM Tris–HCl, pH 8.7, with the ionic strength adjusted by the addition of appropriate salts as indicated in the Figure and Table legends. Initially, we performed G3T unfolding experiments in the presence of 10 mM HEPES pH 7.5; however these final conditions were chosen to study quadruplex stabilities in the buffer conditions suitable for DNA polymerases (50 mM monovalent cations, 2 mM $MgCl_2$). Since all loop positions are equally good for turning on fluorescence signal [17], we investigated the role of loop sequences in GGGAGGGNGGGNGGG and GGGGGGGNGGGNGGG sequences (assuming A and G in the 4th positions as analogs for 2AP and 6MI). In addition, since purine nucleotides in loop positions destabilize the quadruplex [17,22], we employed only T and C in the 8th and 12th positions.

Melting temperatures were determined by recording UV absorption at either 240 nm, 260 nm, or 295 nm as a function of temperature using a Varian UV–visible spectrophotometer (Cary 100 Bio). Fluorescence measurements of 2AP (ex 310 nm, em 370 nm) were performed using a Varian spectrophotometer (Cary Eclipse). Circular dichroism (CD) spectra were obtained with a Jasco-815 spectropolarimeter at using 4 μM oligonucleotide solutions in 1 cm cells. All optical devices were equipped with thermoelectrically-controlled cell holders. In a typical experiment, oligonucleotide samples were mixed and diluted into the desired buffers in optical cuvettes. The solutions were incubated at 95 °C for a few minutes in the cell holder prior to ramping to the desired starting temperature. In the case of DNA duplexes, to ensure that the quadruplex-forming sequence formed a double helix with its complementary strand, the sequences were first annealed in CsCl- and $MgCl_2$-containing buffers. After annealing by heating to 95 °C, the temperature was ramped to the desired starting temperature, KCl was added, and the melting experiments were performed at a heating rate of 0.5 or 1 °C/min. The UV melting curves allowed an estimate of melting temperature, T_m, the midpoint temperature of the unfolding process. van't Hoff enthalpies, ΔH_{vH}, were also calculated using the following equations: $\Delta H_{vH} = 4RT_m^2(\delta\alpha/\delta T)$ in the case of monomolecular quadruplexes and $\Delta H_{vH} = 6RT_m^2(\delta\alpha/\delta T)$ in the case of bimolecular DNA duplexes. R is the gas constant and $\delta\alpha/\delta T$ is the slope of the normalized optical absorbance or fluorescence versus temperature curve at the T_m [23].

Table 1
Melting temperatures (T_m) of the WT G3T quadruplex and variants under different buffer conditions.

Oligonucleotide	Name	T_m (°C)		
		5 mM K^+	10 mM K^+	15 mM K^+
GGG*T*GGG*T*GGG*T*GGG	G3T-*TTT*	84.0	89.0	>94
GGGCGGG*T*GGG*T*GGG	G3T-*CTT*	84.0	88.5	>94
GGGCGGGCGGG*T*GGG	G3T-*CCT*	83.5	88.0	>94
GGGCGGGCGGGCGGG	G3T-*CCC*	82.0	87.0	>94
GCGGG*T*GGG*T*GGG*T*GGG	**GC**-G3T-*TTT*	76.0	82.0	86.0
GCGGGCGGG*T*GGG*T*GGG	**GC**-G3T-*CTT*	76.0	81.5	85.0
GCGGGCGGGCGGG*T*GGG	**GC**-G3T-*CCT*	74.0	81.0	85.0
GCGGGCGGGCGGGCGGG	**GC**-G3T-*CCC*	73.0	79.0	84.0

T_m values (within ±0.5 °C) were derived from UV melting curves measured at a concentration of ~4 μM per strand. Italicized letters indicate the position of loop nucleotides and bold letters correspond to attachments at the 5′-end. All buffers contained 2 mM $MgCl_2$ and 50 mM monovalent cations ($K^+ + Cs^+$).

Table 2
Melting temperatures (T_m) and van't Hoff enthalpies (ΔH_{vH}) derived from UV unfolding profiles of the quadruplexes.

Oligonucleotide	Name	T_m (°C)	ΔH_{vH} (kcal/mol)
GGG*A*GGG*T*GGG*T*GGG	G3T-*ATT*	91.0	55
GGG*A*GGC*C*GG*T*GGG	G3T-*ACT*	91.0	58
GGG*A*GG*T*GGGCGGG	G3T-*ATC*	91.5	55
GGG*A*GGCGGGCGGG	G3T-*ACC*	90.0	54
GGGGGGG*T*GGG*T*GGG	G3T-*GTT*	92.0	56
GGGGGGGCGGG*T*GGG	G3T-*GCT*	91.5	55
GGGGGGG*T*GGGCGGG	G3T-*GTC*	91.5	56
GGGGGGGCGGGCGGG	G3T-*GCC*	91.0	53[a]

T_m values (within ±0.5 °C) and ΔH_{vH} (within ±10%) were derived from UV melting curves at a concentration of ~4 μM per strand; the complex nature of G3T-*GCC* unfolding precluded determination of ΔH_{vH} value. Buffer: 15 mM KCl, 35 mM CsCl, 2 mM $MgCl_2$, 10 mM Tris–HCl, pH 8.7.
[a] Value obtained in the presence of 7 mM KCl.

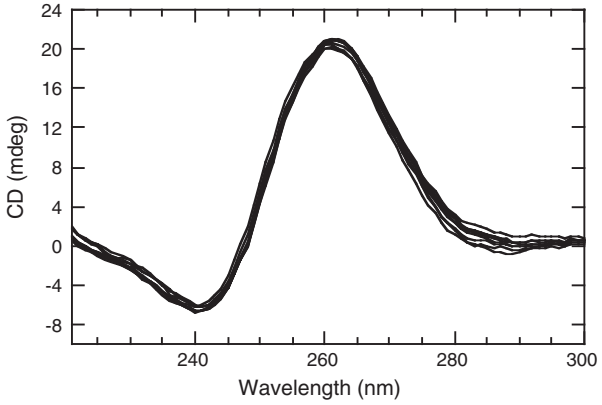

Fig. 1. CD spectra of eight oligonucleotides listed in Table 2. All samples were in 15 mM KCl, 35 mM CsCl, 2 mM $MgCl_2$, 10 mM Tris–HCl pH 8.7 at 20 °C.

3. Results and discussion

3.1. CD measurements

CD spectroscopy has traditionally been used to gain information about the folding topology of DNA quadruplexes. By comparing CD spectra with NMR or X-ray structures of simple DNA quadruplexes containing only G and T nucleotides, the following rules have been established. Parallel quadruplexes, which are structures with all four G-tracts having the same orientation, are characterized by a strong positive peak at ~265 nm and a negative peak of lesser intensity at ~240 nm. Antiparallel quadruplexes demonstrate positive CD bands with maxima at ~245 nm and ~295 nm and a negative peak at ~265 nm [24–26]. The spectra of all quadruplexes studied here are superimposable (Fig. 1) and correspond to parallel folding with a negative peak at 242 nm and positive peak at 262 nm. Thus none of the nucleotide substitutions at loop positions affected the overall conformation of the parallel fold of the G3T quadruplex.

3.2. Unfolding of quadruplexes

Temperature-dependent UV spectroscopy is a convenient tool for studying thermal stability and for estimating van't Hoff thermodynamics of DNA quadruplexes and duplexes. Unfolding of DNA duplexes is usually monitored at 260 nm, while monomolecular quadruplexes can be characterized at 240 and 295 nm [11,27–29]. Initially we recorded the UV spectra of the quadruplex forming sequences in the presence (15 mM KCl, 35 mM CsCl, 2 mM $MgCl_2$) and absence (50 mM CsCl, 2 mM $MgCl_2$) of K^+ ions. The UV difference spectra revealed three peaks at 240 nm, 260 nm and 295 nm [11]. The melting profiles at these wavelengths demonstrate common transitions with the same values of T_m (data not shown). The quadruplex melting curves demonstrated monophasic transition characteristic of a two-state process. To confirm that the transition is a two-state process, an additional dual wavelength test was performed [30]. In particular, plots of the absorbance at a particular wavelength (i.e., 240 nm) versus the absorbance measured at a second wavelength (i.e., 295 nm) were linear (data not shown). This linear dependence, observed for almost all sequences supports the two-state nature of the transition [30]. Only the G3T-*GCC* quadruplex (see Table 2) revealed a premelting process at K^+ concentrations higher than 7 mM, which did not affect the main transition (data not shown). This additional peak could be induced by the formation of intermolecular quadruplexes or non-specific DNA aggregates. Interestingly, the CD profile of G3T-*GCC* measured in the presence of 15 mM K^+ ions (Fig. 1) did not reveal any difference from other sequences, which suggests that the overall secondary structure of the quadruplex is not different from the parallel folds of other quadruplexes.

Initially we performed thermal unfolding experiments of the wild-type (WT) G3T quadruplex (G3T-*TTT*) with T → C substitutions in all positions (Fig. 2 and Table 1). The measurements conducted in the presence of different amounts of K^+ ranging from 5 to 15 mM (Table 1), demonstrate that thermal stability is directly proportional to K^+ concentration. In the presence of the highest K^+ concentration, 15 mM,

Table 3
Melting temperatures (T_m) of DNA duplexes.

Duplex	T_m (°C)		$\Delta T_{m,\ Cs\text{-}K}$ (°C)
	Cs^+	K^+	
G3T-*TTT*	71.5 (68.6)	60.5	11.0
G3T-*CTT*	75.0 (72.3)	66.5	9.5
G3T-*CCT*	78.0 (75.9)	70.0	8.0
G3T-*CCC*	81.5 (79.3)	74.5	7.0
GC-G3T-*TTT*	77.5 (74.3)	68.5	9.0
GC-G3T-*CTT*	79.0 (77.3)	73.0	6.0
GC-G3T-*CCT*	82.0 (80.3)	78.0	4.0
GC-G3T-*CCC*	84.0 (83.1)	82.0	2.0
5′-GGGCGGGCGGG*T*GGGCCCGCCCACCC (G3T-*CT*)	65.5 (61.6)	51.5	14.0
5′-GGGCGGG*T*GGG*T*GGGCCCACCCACCC (G3T-*TT*)	61.5 (55.9)	45.0	16.5
5′-GGG*T*GGG*T*GGGCGGGCCCGCCC (G3T-*C*)	47.0 (36.9)	22.5	24.5

Sequences of one strand of the first eight duplexes are in Table 1. Duplexes were formed by annealing to the complementary strands. Values in parentheses correspond to T_m of the truncated duplexes (missing the last GC base pair) estimated from nearest-neighbor analysis. Measurements were performed either in K^+ buffer (15 mM KCl, 35 mM CsCl, 2 mM $MgCl_2$, 10 mM Tris–HCl, pH 8.7) or in Cs^+ buffer (50 mM CsCl, 2 mM $MgCl_2$, 10 mM Tris–HCl, pH 8.7). $\Delta T_{m,\ Cs\text{-}K}$ corresponds to the T_m difference between duplexes in Cs^+ and K^+ buffers.

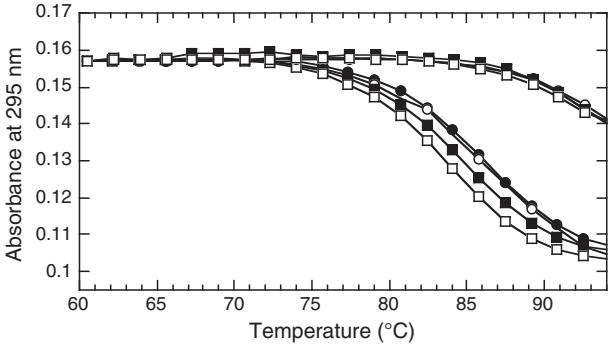

Fig. 2. UV melting profiles of G3T quadruplexes listed in Table 1 measured at 295 nm. Profiles with thermal stabilities ~83 °C correspond to molecules with GC attachments (**GC**-G3T-*TTT* (●), **GC**-G3T-*CTT* (○), **GC**-G3T-*CCT* (□), **GC**-G3T-*CCC* (■)). Incomplete unfolding profiles correspond to molecules without GC attachments. Buffer: 15 mM KCl, 35 mM CsCl, 2 mM $MgCl_2$, 10 mM Tris–HCl pH 8.7.

the quadruplex unfolds ~100 °C, which did not allow us to record a full unfolding profile and determine the exact value of T_m. Various T → C substitutions measured in the presence of 5 and 10 mM K^+ ions (Table 1), did not reveal significant difference in the thermodynamic properties of the quadruplex-forming sequences relative to WT. The data are in good agreement with an earlier study, which revealed only a 2 °C decrease in thermal stability upon all three T → C substitutions and an insignificant decease in ΔH_{vH} [22]. Quadruplexes with GC appended at the 5′-end demonstrated similar behavior: (i) T_m increases with increasing K^+ concentration; and (ii) T → C substitution insignificantly destabilizes the quadruplexes. However, the values of T_m for all molecules are shifted to lower temperatures demonstrating an ~7 °C destabilization effect of a 5′-GC attachment.

A T → A substitution in the 4th position of G3T reveals a significant destabilization effect, ~4 °C, for all four molecules tested (Table 2). Additional T → C substitutions at either position 8 or 12 did not show any measurable effect relative to G3T-*ATT*. Simultaneous T → C substitutions (G3T-*ACC* in Table 2) revealed an ~ 2 °C destabilization effect, which is in good agreement with the present (G3T-*CTT* relative to G3T-*CCC*, Table 1) and published [22] data. T → G substitutions at position 4 (Table 2) are almost identical to the effects of T → A. This might indicate that the destabilization effect is primarily the result of stronger stacking interactions of purine bases with adjacent guanines in the unstructured quadruplex, which has to be overcome during quadruplex formation. The van't Hoff enthalpies, ΔH_{vH}, are similar for all molecules, ~56 kcal/mol (Table 2) and are smaller than those of G3T sequence with all T loops (ΔH_{vH} = 63 kcal/mol) [11]. The difference could be explained by the extra endothermic heat of base-stacking disruption in the present sequences since they contain purine nucleotides in the 4th positions (Table 2).

3.3. Unfolding of duplexes

The primer in QPA is a truncated version of G3T missing one G at the 3′-end. Therefore, it is unable to form a quadruplex and readily anneals to the PBS. Upon polymerase elongation and G addition, the primer dissociates spontaneously and forms a quadruplex. As a result, the PBS is unpaired and ready for the next amplification event. One key feature of QPA is that the primer/PBS complex has to be more stable than the same complex after elongation (quadruplex/PBS complex). Therefore, thermal unfolding experiments were performed for all DNA duplexes listed in Table 3 in the presence and absence of K^+ ions. The T_m values obtained from measurements at 260 nm in Cs^+ buffer (Table 3), agree well with the estimated values from the nearest-neighbor analysis of equilibrium unfolding [31] also listed in Table 3. In the case of K^+ buffer, to ensure that the G3T sequences are duplexed with the complementary strands, the sequences were first annealed in buffer containing all components except 15 mM KCl, which was added later. Melting experiments were conducted at 260 nm (to monitor duplex unfolding) and 295 nm (to monitor quadruplex folding and unfolding). Fig. 3 shows typical unfolding experiments at 295 nm for all duplexes listed in Table 3 in the presence of K^+ buffer. Unfolding of the G3T-*TTT* duplex reveals two transitions: a positive peak with the maximum at 60.5 °C and an incomplete transition above 80 °C (Fig. 3A). The positive peak is the result of unfolding of the duplex and corresponds to the quadruplex formation of the released G3T sequences. The quadruplex unfolds above 80 °C, which is accompanied by a decrease at 295 nm and coincides with the melting curves of quadruplexes alone (Fig. 2). As expected, simultaneous monitoring of the unfolding experiment at 260 nm revealed only duplex unfolding at 60.5 °C (data not shown). Thus, duplex unfolding monitored both by (i) direct measurement at 260 nm and (ii) quadruplex formation upon duplex unfolding monitored at 295 nm, reveals the same results. The T → C substitutions shifted the positive peaks to higher temperatures, while quadruplex unfolding was unaffected (Fig. 3A and Table 3).

GC attachment to G3T-*TTT* significantly changes the melting profile and reveals two successive transitions: (i) duplex unfolding, which is shifted by 8 °C due to the stabilization effect of two extra G·C base pairs; and (ii) quadruplex unfolding, with a T_m at ~85 °C. The decrease in quadruplex T_m is induced by a destabilization effect of GC attachment at the 5′-end (Fig. 2, Table 1). As expected, the T → C substitutions in **GC**-G3T-*TTT* increase duplex stability, which results in overlapping duplex and quadruplex unfolding processes (Fig. 3B). Unfolding profiles of 11-bp and 7-bp duplexes also demonstrate two separate transitions for each duplex (Fig. 3C). As expected, thermal stabilities of the duplexes are shifted to lower temperatures, while T_m values of quadruplexes are not affected (see Fig. 3A).

Inspection of Table 3 reveals that the presence of K^+ ions has a destabilizing effect on all duplexes. For instance, in Cs^+ buffer G3T-*TTT* unfolds at 71.5 °C, while in K^+ buffer thermal stability decreases to 60.5 °C. The destabilization is due to the non-equilibrium nature of the transition in the presence of quadruplex-forming K^+ ions; unfolding of the duplex is accompanied by quadruplex formation of the released strands, which inhibits the reverse reaction (duplex refolding) and as a result, shifts it to lower temperatures. Previous UV melting experiments of the G3T duplex in the presence of K^+ ions performed at slower heating rates (0.5 °C/min and 0.1 °C/min) shifted the transition to lower temperatures [14], which further supports the non-equilibrium nature of the transition. The highest destabilization, 24.5 °C, is observed for the least stable 7-bp duplex and the lowest destabilization, 3 °C, is observed for the most stable duplex, **GC**-G3T-*CCC*. The destabilizing effect is inversely proportional to T_m values of the duplexes and is determined by the thermal stability of the quadruplexes (Fig. 4). The plot reveals two linear functions. The first one corresponds to DNA duplexes containing quadruplexes with GC extensions and has a y-intercept of 86.5 °C and a slope of −1.2. A second transition is observed for the duplexes without a 5′-GC extension, and has a y-intercept of 93.5 °C

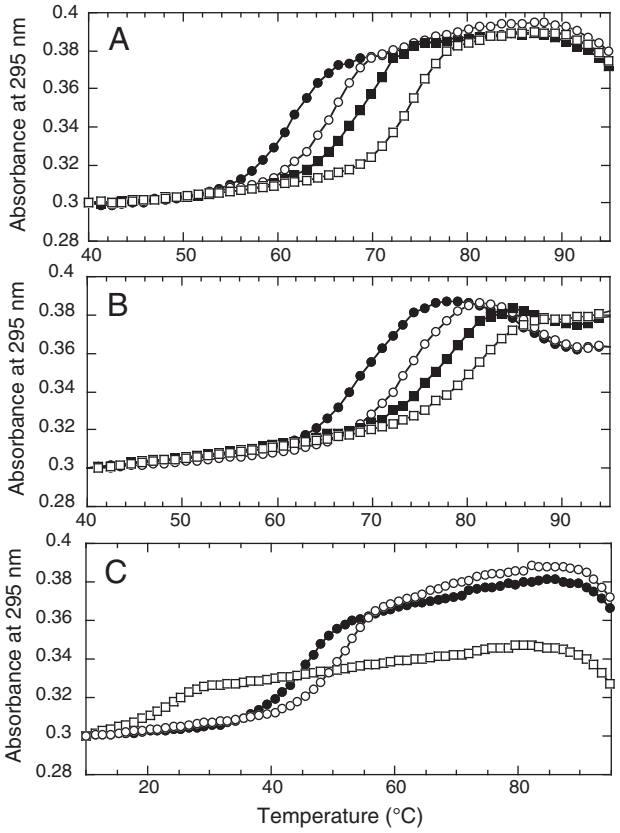

Fig. 3. UV melting profiles of duplexes listed in Table 3 monitored at 295 nm. (A) G3T-*TTT* (●), G3T-*CTT* (○), G3T-*CCT* (□), G3T-*CCC* (■); (B) **GC**-G3T-*TTT* (●), **GC**-G3T-*CTT* (○), **GC**-G3T-*CCT* (□), **GC**-G3T-*CCC* (■); (C) G3T-*CT* (○),G3T-*TT* (●) and G3T-*C* (□). Buffer: 15 mM KCl, 35 mM CsCl, 2 mM $MgCl_2$, 10 mM Tris–HCl pH 8.7.

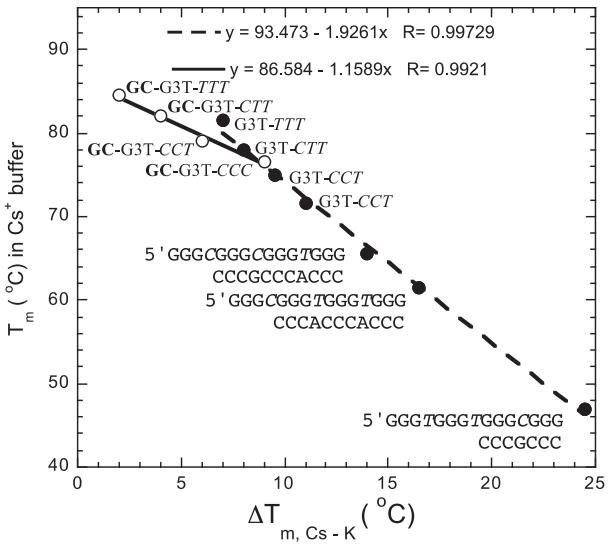

Fig. 4. Correlation of T_m values of the quadruplexes with $\Delta T_{m,\ Cs\text{-}K}$ values (see Table 3).

and a slope of −1.9. These two transitions reflect the fact that thermal stabilities of G3T-*TTT* or **GC**-G3T-*TTT* quadruplexes are insensitive to T → C substitutions, while significant destabilization is induced by the 5′-GC extension. Interestingly, the values of the y-intercepts are approximately equal to the T_m of the corresponding quadruplexes, ~85 °C and 94 °C (see Table 1). This supports the conclusion that QPA is driven by the free energy of quadruplex formation.

As mentioned above, the initial primer/PBS duplex has to be more stable than the duplex after elongation (quadruplex/PBS complex). The thermal stabilities of primer/PBS complexes shown in parentheses (Table 3) are greater than the quadruplex/PBS stabilities, measured in K^+ for all molecules. Thus all the systems described here are suitable for isothermal QPA.

4. Conclusions

We systematically studied the thermodynamic and optical properties of the WT G3T quadruplex and variants containing sequence modifications in loop positions and extensions at the 5′-end. CD studies revealed that the substitution of thymidines or GC addition to the 5′-end does not affect the parallel fold of the quadruplex. Thermal unfolding experiments demonstrated that purine bases incorporated at loop positions and 5′-end dinucleotide extension significantly destabilize the quadruplex, while loop pyrimidines have almost no effect. The results of this study indicate that linear isothermal QPA can be performed over a wide temperature range (40–80 °C) suitable for both thermophilic and mesophilic DNA polymerases.

Acknowledgments

This work was funded by a grant from the Bill & Melinda Gates Foundation through the Grand Challenges in Global Health initiative. Levan Lomidze and David Gvarjaladze were supported by a grant (DI/23/7-230/12) from Shota Rustaveli National Science Foundation (Georgia).

References

[1] M.L. Bochman, K. Paeschke, V.A. Zakian, DNA secondary structures: stability and function of G-quadruplex structures, Nat. Rev. Genet. 13 (2012) 770–780.
[2] A. De Cian, G. Cristofari, P. Reichenbach, E. De Lemos, D. Monchaud, M.P. Teulade-Fichou, K. Shin-Ya, L. Lacroix, J. Lingner, J.L. Mergny, Reevaluation of telomerase inhibition by quadruplex ligands and their mechanisms of action, Proc. Natl. Acad. Sci. U. S. A. 104 (2007) 17347–17352.
[3] R.D. Gray, L. Petraccone, J.O. Trent, J.B. Chaires, Characterization of a K+-induced conformational switch in a human telomeric DNA oligonucleotide using 2-aminopurine fluorescence, Biochemistry 49 (2010) 179–194.
[4] N. Maizels, Dynamic roles for G4 DNA in the biology of eukaryotic cells, Nat. Struct. Mol. Biol. 13 (2006) 1055–1059.
[5] D. Piekna-Przybylska, G. Sharma, R.A. Bambara, Mechanism of HIV-1 RNA dimerization in the central region of the genome and significance for viral evolution, J. Biol. Chem. 288 (2013) 24140–24150.
[6] C. Schaffitzel, I. Berger, J. Postberg, J. Hanes, H.J. Lipps, A. Pluckthun, In vitro generated antibodies specific for telomeric guanine-quadruplex DNA react with *Stylonychia lemnae* macronuclei, Proc. Natl. Acad. Sci. U. S. A. 98 (2001) 8572–8577.
[7] L.C. Bock, L.C. Griffin, J.A. Latham, E.H. Vermaas, J.J. Toole, Selection of single-stranded DNA molecules that bind and inhibit human thrombin, Nature 355 (1992) 564–566.
[8] N. Jing, C. Marchand, J. Liu, R. Mitra, M.E. Hogan, Y. Pommier, Mechanism of inhibition of HIV-1 integrase by G-tetrad-forming oligonucleotides in vitro, J. Biol. Chem. 275 (2000) 21460–21467.
[9] R.F. Rando, J. Ojwang, A. Elbaggari, G.R. Reyes, R. Tinder, M.S. McGrath, M.E. Hogan, Suppression of human immunodeficiency virus type 1 activity in vitro by oligonucleotides which form intramolecular tetrads, J. Biol. Chem. 270 (1995) 1754–1760.
[10] H.M. So, K. Won, Y.H. Kim, B.K. Kim, B.H. Ryu, P.S. Na, H. Kim, J.O. Lee, Single-walled carbon nanotube biosensors using aptamers as molecular recognition elements, J. Am. Chem. Soc. 127 (2005) 11906–11907.
[11] S. Kelley, S. Boroda, K. Musier-Forsyth, B.I. Kankia, HIV-integrase aptamer folds into a parallel quadruplex: a thermodynamic study, Biophys. Chem. 155 (2011) 82–88.
[12] N. Jing, R.F. Rando, Y. Pommier, M.E. Hogan, Ion selective folding of loop domains in a potent anti-HIV oligonucleotide, Biochemistry 36 (1997) 12498–12505.
[13] N.Q. Do, K.W. Lim, M.H. Teo, B. Heddi, A.T. Phan, Stacking of G-quadruplexes: NMR structure of a G-rich oligonucleotide with potential anti-HIV and anticancer activity, Nucleic Acids Res. 39 (2011) 9448–9457.
[14] B.I. Kankia, Self-dissociative primers for nucleic acid amplification and detection based on DNA quadruplexes with intrinsic fluorescence, Anal. Biochem. 409 (2011) 59–65.
[15] A. Taylor, A. Joseph, R. Okyere, S. Gogichaishvili, K. Musier-Forsyth, B. Kankia, Isothermal quadruplex priming amplification for DNA-based diagnostics, Biophys. Chem. 171 (2013) 1–8.
[16] A. Niemz, T.M. Ferguson, D.S. Boyle, Point-of-care nucleic acid testing for infectious diseases, Trends Biotechnol. 29 (2011) 240–250.
[17] J. Johnson, R. Okyere, A. Joseph, K. Musier-Forsyth, B. Kankia, Quadruplex formation as a molecular switch to turn on intrinsically fluorescent nucleotide analogs, Nucleic Acids Res. 41 (2013) 220–228.
[18] S.M. Law, R. Eritja, M.F. Goodman, K.J. Breslauer, Spectroscopic and calorimetric characterizations of DNA duplexes containing 2-aminopurine, Biochemistry 35 (1996) 12329–12337.
[19] L.W. McLaughlin, T. Leong, F. Benseler, N. Piel, A new approach to the synthesis of a protected 2-aminopurine derivative and its incorporation into oligodeoxynucleotides containing the Eco RI and Bam HI recognition sites, Nucleic Acids Res. 16 (1988) 5631–5644.
[20] M.E. Hawkins, Fluorescent pteridine probes for nucleic acid analysis, Methods Enzymol. 450 (2008) 201–231.
[21] B.I. Kankia, L.A. Marky, DNA, RNA, and DNA/RNA oligomer duplexes: a comparative study of their stability, heat, hydration and Mg(2+) binding properties, J. Phys. Chem. B 103 (1999) 8759–8767.
[22] P.A. Rachwal, T. Brown, K.R. Fox, Sequence effects of single base loops in intramolecular quadruplex DNA, FEBS Lett. 581 (2007) 1657–1660.
[23] L.A. Marky, K.J. Breslauer, Calculating thermodynamic data for transitions of any molecularity from equilibrium melting curves, Biopolymers 26 (1987) 1601–1620.
[24] A. Matsugami, K. Ouhashi, M. Kanagawa, H. Liu, S. Kanagawa, S. Uesugi, M. Katahira, An intramolecular quadruplex of (GGA)(4) triplet repeat DNA with a G:G:G:G tetrad and a G(:A):G(:A):G(:A):G heptad, and its dimeric interaction, J. Mol. Biol. 313 (2001) 255–269.
[25] S. Paramasivan, I. Rujan, P.H. Bolton, Circular dichroism of quadruplex DNAs: applications to structure, cation effects and ligand binding, Methods 43 (2007) 324–331.
[26] C.F. Tang, R.H. Shafer, Engineering the quadruplex fold: nucleoside conformation determines both folding topology and molecularity in guanine quadruplexes, J. Am. Chem. Soc. 128 (2006) 5966–5973.
[27] B.I. Kankia, Optical absorption assay for strand-exchange reactions in unlabeled nucleic acids, Nucleic Acids Res. 32 (2004) e154.
[28] B.I. Kankia, L.A. Marky, Folding of the thrombin aptamer into a G-quadruplex with Sr(2+): stability, heat, and hydration, J. Am. Chem. Soc. 123 (2001) 10799–10804.
[29] J.L. Mergny, A.T. Phan, L. Lacroix, Following G-quartet formation by UV-spectroscopy, FEBS Lett. 435 (1998) 74–78.
[30] P. Wallimann, R.J. Kennedy, J.S. Miller, W. Shalongo, D.S. Kemp, Dual wavelength parametric test of two-state models for circular dichroism spectra of helical polypeptides: anomalous dichroic properties of alanine-rich peptides, J. Am. Chem. Soc. 125 (2003) 1203–1220.
[31] M. Zuker, Mfold web server for nucleic acid folding and hybridization prediction, Nucleic Acids Res. 31 (2003) 3406–3415.